



## Mechanical effect of double-level degeneration of lumbar spine discs by finite element method

A. Orang<sup>1</sup>, M. Haghghi-Yazdi<sup>1,\*</sup>, S. R. Mehrpour<sup>2</sup>

<sup>1</sup> School of Mechanical Engineering, College of Engineering, University of Tehran, Tehran, Iran

<sup>2</sup> Medical Department, Tehran University of Medical Sciences, Tehran, Iran

**ABSTRACT:** This study intends to present a biomechanical model of the lumbar spine applying the finite element method in order to evaluate the behavior of the spine with disc degeneration. The high rates of patients suffering from this phenomenon encouraged us to study the effects of disc degeneration on spinal response. In the proposed method, the entire lumbar spine, including the vertebrae L1 to S1, were simulated. Degeneration of the disc was also modeled in three different ways, decreasing disc height, changing the mechanical properties of the nucleus, and changing the properties of ligaments and collagen fibers. This degeneration was considered simultaneously for both L4-5 and L5-S1 discs, which is referred to as double-level degeneration in this study. After modeling and applying synthetic loading (bending moments with a follower load), the analysis was performed via ABAQUS software. The results, including intradiscal pressures and the intervertebral rotation, were also compared with experimental data for further verification. The findings of this study illustrate that double-level disc degeneration reduces intradiscal pressures in L4-5 and L5-S1 discs. However, the intradiscal pressure of a degenerated disc does not change the intradiscal pressure of other adjacent discs. Moreover, in extension and axial rotation loading, increasing disc degeneration would lead to an increase in intervertebral motion.

### Review History:

Received: 28/05/2019

Revised: 15/05/2020

Accepted: 21/06/2020

Available Online: 01/07/2020

### Keywords:

Finite Element Model

Lumbar Spine

Disc Degeneration

Intradiscal Pressure

Intervertebral Rotation

## 1. INTRODUCTION

Disc degeneration is a natural process that is caused mainly by aging. Degeneration is usually accompanied by a change in the appearance and chemical structure of the disc. These biological changes in the structure of the disc can lead to back pain which is one of the most common problems people encounter throughout the world. This disease can generate many problems in the social, economic, and working conditions of individuals. Around 80 percent of people at the age of fifty suffer from back pain, although at such younger ages, it might have also emerged [1, 2]. Disc degeneration is also known to be one of the most common causes of acute and chronic back pains and can arise in different degrees. In about 98% of cases, it has been observed between L4-L5 vertebrae and it has been less observed in L5-S1 and L3-L4. Although this process might occur at any age, it mostly happens to males at ages between 50 to 70 years old [3].

Geometric complexity, complex material behavior, various boundary conditions as well as loading variations in problems involving simulation of spine behavior make achieving an accurate solution to such problems very difficult. Applying approximate solutions with acceptable accuracy, which could be conducted in a reasonable time scale, seems a great solution to these problems. The finite Element Method (FEM) is one of the best choices in this regard. The advantage of FEM in studying the biomechanics

of the spine is its capability in combining three-dimensional vertebrae geometry, complex constraints, loading conditions, as well as material nonlinearity and anisotropy.

Numerous finite element models have been developed to investigate the disc degeneration of one Functional Spinal Unit (FSU) of the lumbar spine, including simple models [4-6] and complicated models [7] in terms of the geometry as well as the constituents. The trend of Range Of Motion (ROM), IntraDiscal Pressure (IDP), and Facet Joint Force (FJF) observed in these studies has been different. Rohlmann et al. [8] have reached the conclusion that the progression of disc degeneration has increased ROM for all cases of loading. This is while Schmidt et al. [7] has found out that the progression of disc degeneration causes an increase in ROM for loading cases of flexion (FLX)-extension (EXT) and Lateral Bending (LB); but reduces ROM in LB loading. This is in agreement with the experimental results of Brown et al. [9]. In both of these studies [7, 8], in all cases of loading, the progression of disc degeneration induces a declining trend in IDP and a rising trend in FJF. A few studies were also devoted to the modeling of the whole lumbar spine to investigate the results of ROM, IDP, and FJF [4, 10, 11]. In the study of Park et al. [12], where the whole lumbar spine has also been modeled, it has been seen that in all loading cases, IDP has decreased with the progression of degeneration. However, FJF has experienced an increasing trend in LB and Axial Rotation (AR) but has decreased in EXT loading cases. In

\*Corresponding author's email: mohaghghi@ut.ac.ir



the study of Wu et al. [13], double degeneration for the lower lumbar spine (L3-S1) has also been studied. However, in the results section of their study, only the ROM results for the three modes of degeneration (mild, moderate, and severe) have been studied and no other parameters related to lumbar spine response such as IDP and FJF have been presented. Also, the follower load has not been used to minimize spinal movement and improve spinal pressure stability without muscle. The verification of the results for the case of ROM has been only done with in-vitro data. The above-mentioned points are the limitations of the study of Wu et al. [13] and in the present study these limitations are completely addressed.

Our main motivation for conducting the current research work was the high percentage of patients with double-level disc degeneration. Based on a study by Kanna et al. [14], patients aged between 20 to 50 years old were studied in terms of disc degeneration in two categories: i) 91 patients having disc prolapse, and ii) 133 patients with disc degeneration. 45 patients in the second category (33.8%) had single-level disc degeneration, and 25 patients (18.8%) had contiguous double-level degeneration, and only 4 patients (3%) had non-contiguous double-level degeneration. This is while 94% of the degeneration in the 25 patients suffering contiguous double-level degeneration was related to L4-L5 and L5-S1 discs. Also, in another study [15] that considered 262 patients, 94 patients had no disc degeneration; 99 patients had single-level degeneration (28 patients had L4-L5 disc degeneration and 71 had L5-S1 disc degeneration), and 69 patients (26%) had double-level disc degeneration in L4-L5-S1 discs. These two research studies show that the number of patients suffering double-level disc degeneration in L4-L5-S1 discs is almost equal to that of single-level disc degeneration.

To the best knowledge of the authors, the effect of double-level degeneration has yet to be studied for the entire lumbar spine. Therefore, the current study involves considering the degeneration of two adjacent discs; i.e., L5-S1 and L4-L5 discs and their effect is studied by examining the IDP, ROM and FJF of entire discs. The following sections include lumbar spine modeling and material specifications, validating the model with in-vitro data, and finally presenting ROM, IDP, and FJF results.

## 2. MATERIALS AND METHODS

### 2.1. 3d Geometry Acquisition

Three-dimensional geometry of the bone structure, which consists of L1 to S1 vertebrae, has been reconstructed from a 0.75-mm thick CT scan of a 26-year-old male healthy person. The division was performed using the Mimics (MIMICS Research 17.0, Materialise, Belgium) medical image processing software. Then, the geometry was cleaned from spikes and sharp edges using the software Geomagic Studio (Geomagic Studio 2014, 3D systems, USA) (Fig. 1(a)).

The obtained geometry was then meshed using the software package of Hypermesh (Hyperworks 12.0, Altair, USA) (Fig. 1(b)). The cortical bone and endplates were meshed using 3-node shell elements with a uniform thickness of 1 mm. The cortical bone was then filled with 4-node

(tetrahedral) solid elements to represent the cancellous core. The mesh of two intervening endplates was used to create the disc by extruding 7 circumferential layers of solid elements for the annulus fibrosus ground enclosing the nucleus mesh (Fig. 1(c)) [16, 17].

These layers were reinforced by unidirectional springs distributed in concentric lamellae with crosswise pattern close to  $\pm 30^\circ$  to represent the annular fibers (Fig. 1(c)). The disc volume was divided with a proportion according to the histological findings (44%\_nucleus and 56%\_annulus) [16, 18].

The ligaments include the Anterior Longitudinal Ligament (ALL), Posterior Longitudinal Ligament (PLL), Capsular Ligament (CL), Intertransverse Ligament (ITL), Ligamentum Flavium (LF), Supraspinous Ligament (SSL), and Interspinous Ligament (ISL), which were all modeled by unidirectional springs [19]. Facet joint modeling is a surface-to-surface contact with no friction with the same amount of gap observed in the CT scan image without any change [20]. A fine mesh particularly in the facet joints areas was used to ensure the accuracy of the predicted response [21].

#### 2.1.1. Material Properties

The behavior of the bony structures and cartilaginous endplates was assumed linear elastic (where  $E$  and  $\nu$  are Young's modulus and Poisson's ratio, respectively) while the annulus and nucleus behaviors were both governed by hyperelastic material law using the first-order of Mooney–Rivlin formulation. The material properties of the spinal components are summarized in Table 1.

Nonlinear force-deflection curves adopted from Naserkhaki et al. [23] (Table 2) were assigned to the ligament springs to resist tension only. The annular fibres had nonlinear force-displacement relationship with stiffness increasing from inner to outer lamella [24, 25]. In previous studies, the properties of collagen fibers have been used in the models, but no detailed information is provided. Collagen fibers are different in each layer; both in terms of the number (low to high cross-sections from inner towards outer layers) and also the properties (lower stiffness to higher stiffness from inner to outer layers). Also, how the fibers are distributed in a single layer is not clear yet. The first paper that presented part of these details is the study by Shirazi-adl et al. back in 1984 and 1986 [26]. Most of the subsequent models adopted the fibers properties from the work of Shirazi-adl et al. [26] but other details such as cross-section, stiffness, and the distribution are not mentioned in any of these studies.

#### 2.1.2. Loading And Boundary Conditions

The FE analyses were conducted using the implicit solver of ABAQUS (ABAQUS 6.14, Dassault Systems Simulia Corp., USA). To minimize spinal movement and improve spinal pressure stability without muscle, a compressive force of 100 N is applied. The line of action of this force extends along the curvature of the spine and passes through the vertebral bodies centroids [27, 28]. This Follower Load (FL) was applied using pre-compressed unidirectional

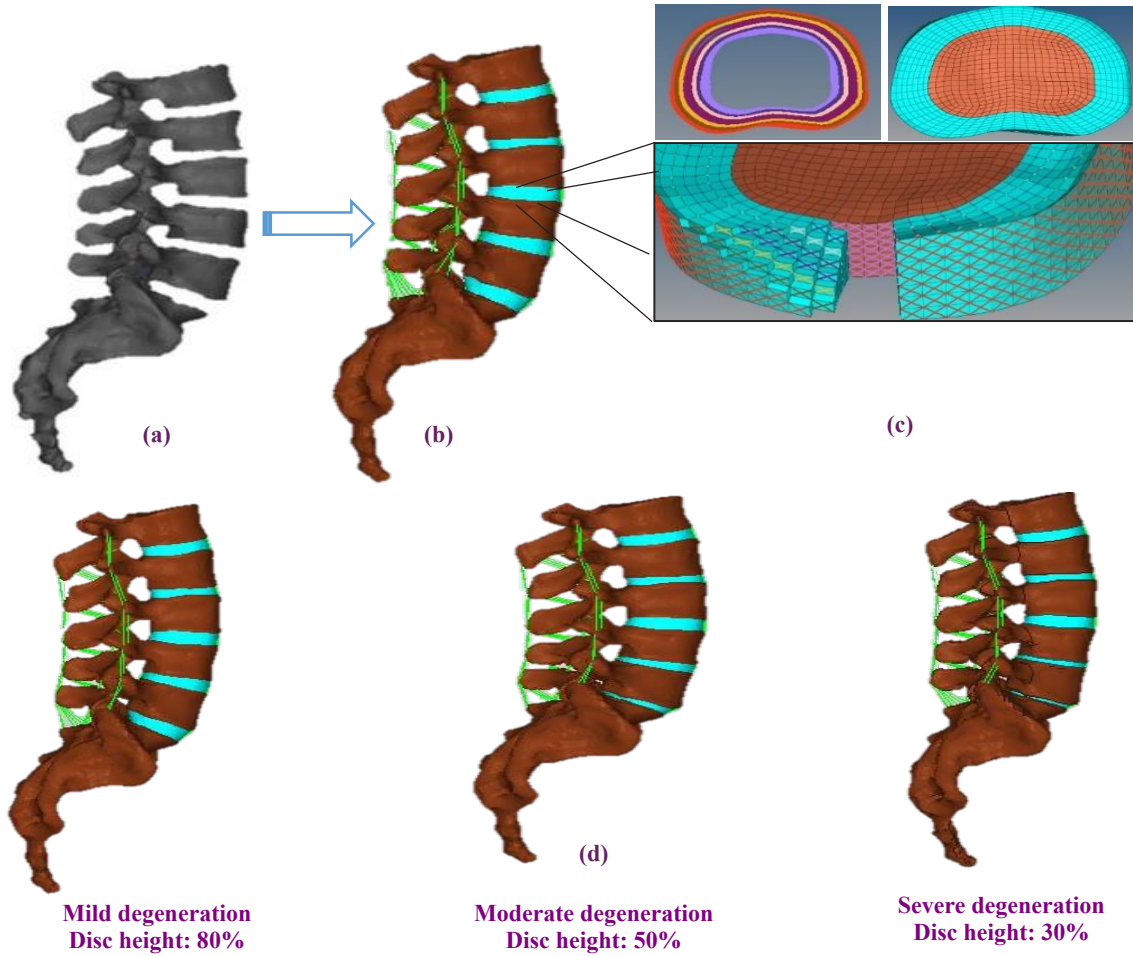


Fig. 1. Step-by-step FE model creation (a) 3D reconstruction (segmentation) and cleaning of the bony elements (b) Mesh generation and material properties assignment (c) Disc meshing details (d) Three double-level degeneration types for L4-L5 and L5-S1 discs.

Table 1. Material properties of the spinal components

Spinal components	Mechanical properties	Material behavior	References
Cortical bone	$E = 12000$ (MPa) $\nu = 0.30$	Linear elastic	[22]
Cancellous bone	$E = 200$ (MPa) $\nu = 0.25$	Linear elastic	
Cartilaginous endplate	$E = 23.8$ (MPa) $\nu = 0.40$	Linear elastic	
Annulus ground substance	$C10 = 0.18$ $C01 = 0.045$	Hyper-Elastic	
Nucleus pulposus	$C10 = 0.12$ $C01 = 0.03$	Hyper-Elastic	

springs inserted between the centroids of two adjacent vertebral bodies [29] Loading is performed in five different modes of flexion, extension, lateral bending, axial rotation, and combined loading. Combined loading includes the combination of one of the four load modes of FLX, EXT, LB, and AR with FL. The load is applied uniformly to the upper endplate L1. The S1 vertebra is also fixed (without moving in each of the six degrees-of-freedom).

In this study, two different finite element models have not been developed. One main model includes the lumbar spine involving L1 to S1 vertebrae, where the geometry is modeled based on the CT scan of a 26-year-old male healthy person. This is different from in-vitro geometries and those of numerical studies, considering that the similarities and differences are difficult to compare. This is while the L4-L5 model is not new, but a segment of L1-S1 lumbar model, where L1 to L3 and S1 vertebrae with the corresponding discs were eliminated from the main lumbar model.

The boundary condition of both L1-S1 lumbar model

and L4-L5 segment includes constrained condition (fully clamped) at the lower endplate of S1 and L5 vertebrae, respectively. This kind of boundary condition exactly matches with that used in in-vitro samples as well as that of numerical studies. The moment has also been applied on L1 and L4 vertebrae in L1-S1 main lumbar model and L4-L5 segment, respectively. This loading type is also the same as that used in in-vitro and numerical models. Since static analyses were used in the current study, even if L1 to L3 vertebrae and the corresponding discs were not removed from the main model and the moment was applied on L4 vertebra of the main model, the same result would be obtained. However, a new L4-L5 model was developed to improve computational efficiency.

Nevertheless, this limitation always exists that in-vitro studies are very limited [1-3] and all geometrical and material properties of these samples are not detectable. The properties have not been reported even if they are detectable. Therefore, it is quite acceptable that the geometrical and

**Table 2. Properties of ligaments in the lumbar spine**

Ligaments	Strain	Stiffness	Strain	Stiffness	Strain	Stiffness	Strain	Stiffness
	(%)	(N/mm)	(%)	(N/mm)	(%)	(N/mm)	(%)	(N/mm)
ALL	$\epsilon < 0$	0	$0 < \epsilon < 12.2$	347	$12.2 < \epsilon < 20.3$	787	$20.3 < \epsilon$	1864
PLL			$0 < \epsilon < 11.1$	29.5	$11.1 < \epsilon < 23$	61.7	$23 < \epsilon$	236
CL			$0 < \epsilon < 25$	36	$25 < \epsilon < 30$	159	$30 < \epsilon$	384
ITL			$0 < \epsilon < 18.2$	0.3	$18.2 < \epsilon < 23.3$	1.8	$23.3 < \epsilon$	10.7
LF			$0 < \epsilon < 5.9$	7.7	$5.9 < \epsilon < 49$	9.6	$49 < \epsilon$	58.2
SSL			$0 < \epsilon < 20$	2.5	$20 < \epsilon < 25$	5.3	$25 < \epsilon$	34
ISL			$0 < \epsilon < 13.9$	1.4	$13.9 < \epsilon < 20$	1.5	$20 < \epsilon$	14.7

**Table 3. Nucleus pulposus properties of the 3 types of degeneration**

Disc Components	Mechanical properties
Nucleus pulposus (mild)	C10 = 0.14 C01 = 0.035
Nucleus pulposus (moderate)	C10 = 0.17 C01 = 0.041
Nucleus pulposus (severe)	C10 = 0.19 C01 = 0.045

material properties of the developed models are not the same as those of in-vitro samples. The comparisons are then made with a wide range of response data. However, the loading and boundary conditions of all developed models are the same as those used in in-vitro tests.

In-vitro studies that deal with the behavior of the lumbar spine or segments have not been devoted to material properties characterization and therefore, do not present any findings. Although there are other in-vitro studies that have specifically determined material properties that have a wide range.

**Table 4. Offset values for the non-linear force-deflection curves in mm**

	mild	moderate	severe
Annulus fibers	0.72 (average)	1.68 (average)	2.56 (average)
ALL	-1.04	1.76	2.72
PLL	-0.32	2.8	4.16
CL	1.1	1.7	4.4
ITL	0.49	1.29	1.8
LF	0.36	1.02	1.74
SSL	0.15	-0.25	-1.3
ISL	1.4	3.2	4.91

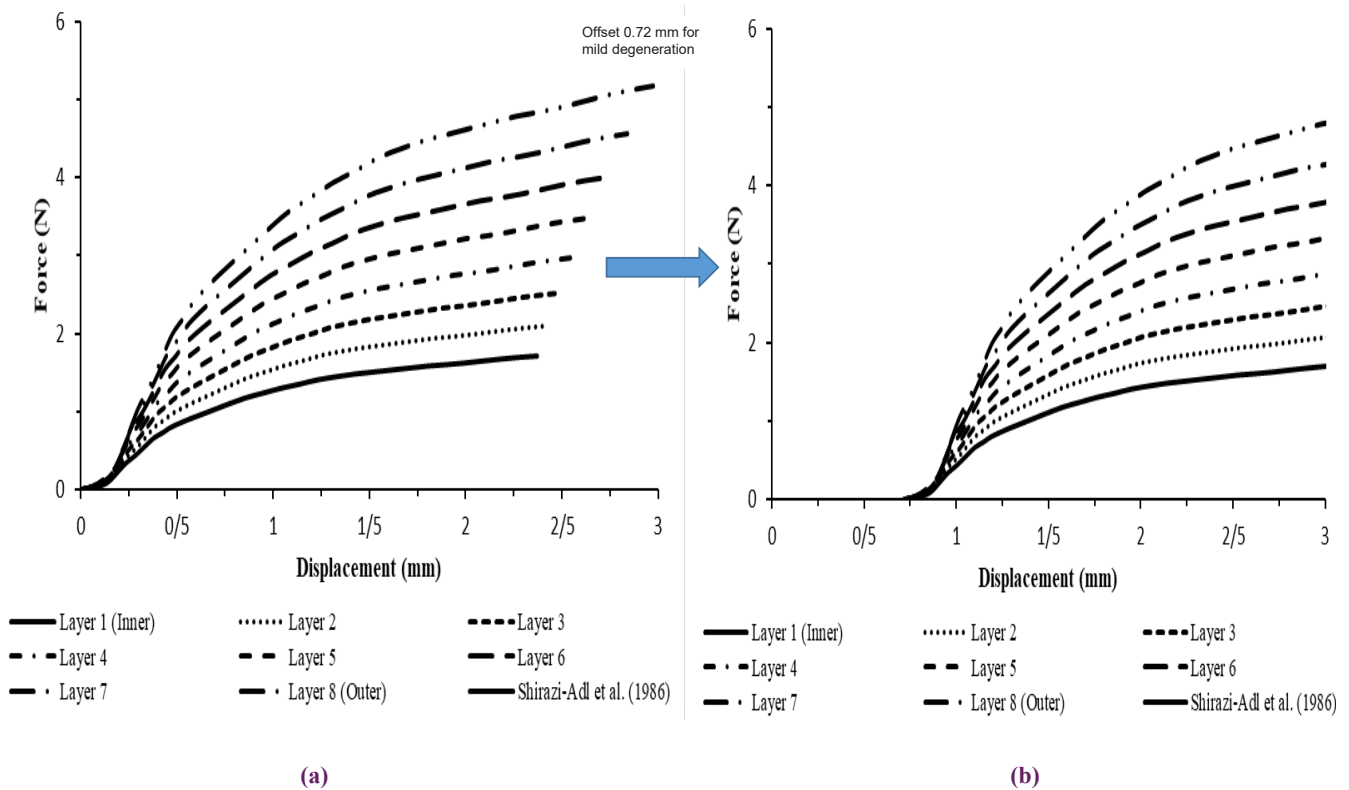


**Fig. 2 (a) is used for collagen fiber properties in L4-L5 intact disc. This is while this curve is shifted 0.72 mm to the right to represent the same properties for mild degeneration (Fig. 2(b)).**

## Mesh convergence For L4-5 intact in M=10 N.m

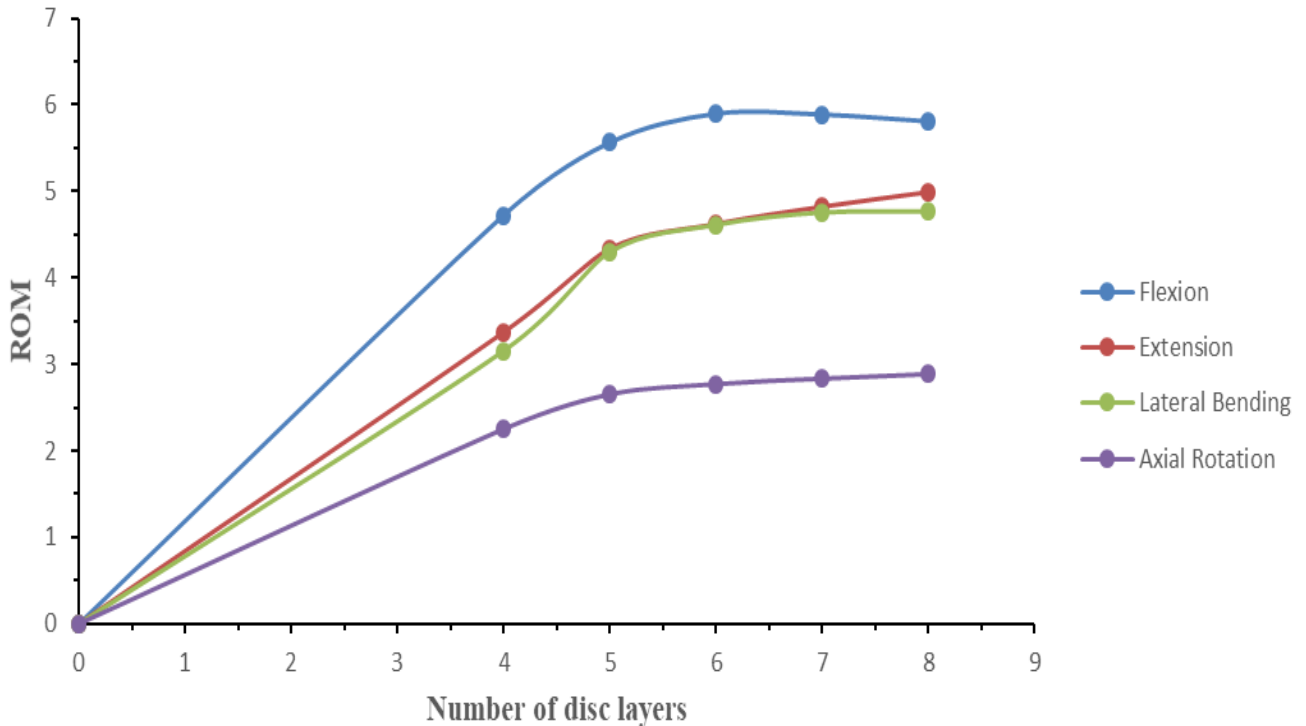


Fig. 3. Mesh convergence study for L4-L5 segment model.

### 2.2. Degeneration Model

This study has modeled disc degeneration by reducing disc height and changing the properties of the nucleus, ligaments, and collagen fibers. Based on the study of Wilke et al. [30], height reduction is categorized in three different types of degeneration: mild condition (height reduction < 33%), moderate condition (33% < height reduction < 66%) and severe condition (height reduction > 66%). Height reduction for three degeneration types was considered as 30%, 50% and 80%, respectively (Fig. 1d).

Changing the properties of the nucleus is based on the amount of degeneration results obtained from the experimental study of Schmidt et al. [7]. The material properties of the disc components in three different types of degeneration is hyper-elastic which were meshed using 3D solid elements. The coefficients  $C10$  and  $C01$  for the three different degeneration types are tabulated in Table 3.

Changing the properties of ligaments and collagen fibers considering offset of the nonlinear force-displacement curve is given in Table 4 [7]. It is indicated in the study of Schmidt et al. [7] that assigning the properties of ligaments and collagen fibers in a degenerated disc can be accomplished by offsetting

the force-displacement curve. Decrease of disc height due to degeneration may cause buckling behavior in the fibers and most of the ligaments [8]. As presented in the finite element modeling of Rohlmann et al. [8], the length change of the fibers due to buckling can be modeled by offsetting their non-linear force-displacement curves (Table 4). To explain this offsetting, an example is given below.

Fig. 2 (a) is used for collagen fiber properties in L4-L5 intact disc. This is while this curve is shifted 0.72 mm to the right to represent the same properties for mild degeneration (Fig. 2(b)).

### 2.3. Mesh Sensitivity Analysis

To ensure that the predictions of the model were unaffected by the mesh resolution, mesh refinement was verified. Five different mesh size is considered for L4-L5 segment, by which validation study was also conducted in this study. Since the elements of the vertebra do not affect the results and in most studies, the vertebra is considered rigid to reduce the computational cost, the number of elements related to disc is only changed in this study. Therefore, disc layers through the height are changed to study the convergence of the model

**Table 5. The effect of mesh size on ROM in different loading cases at 10 N.m moment**

number of layers (number of elements)	ROM in FLX (10 N.m)	ROM in EXT (10 N.m)	ROM in LB (10 N.m)	ROM in AR (10 N.m)
4 (97942)	4.723	3.372	3.156	2.251
5 (99734)	5.564	4.338	4.3	2.652
6 (101523)	5.897	4.623	4.613	2.771
7 (104962)	5.887	4.822	4.755	2.834
8 (105110)	5.808	4.991	4.765	2.886

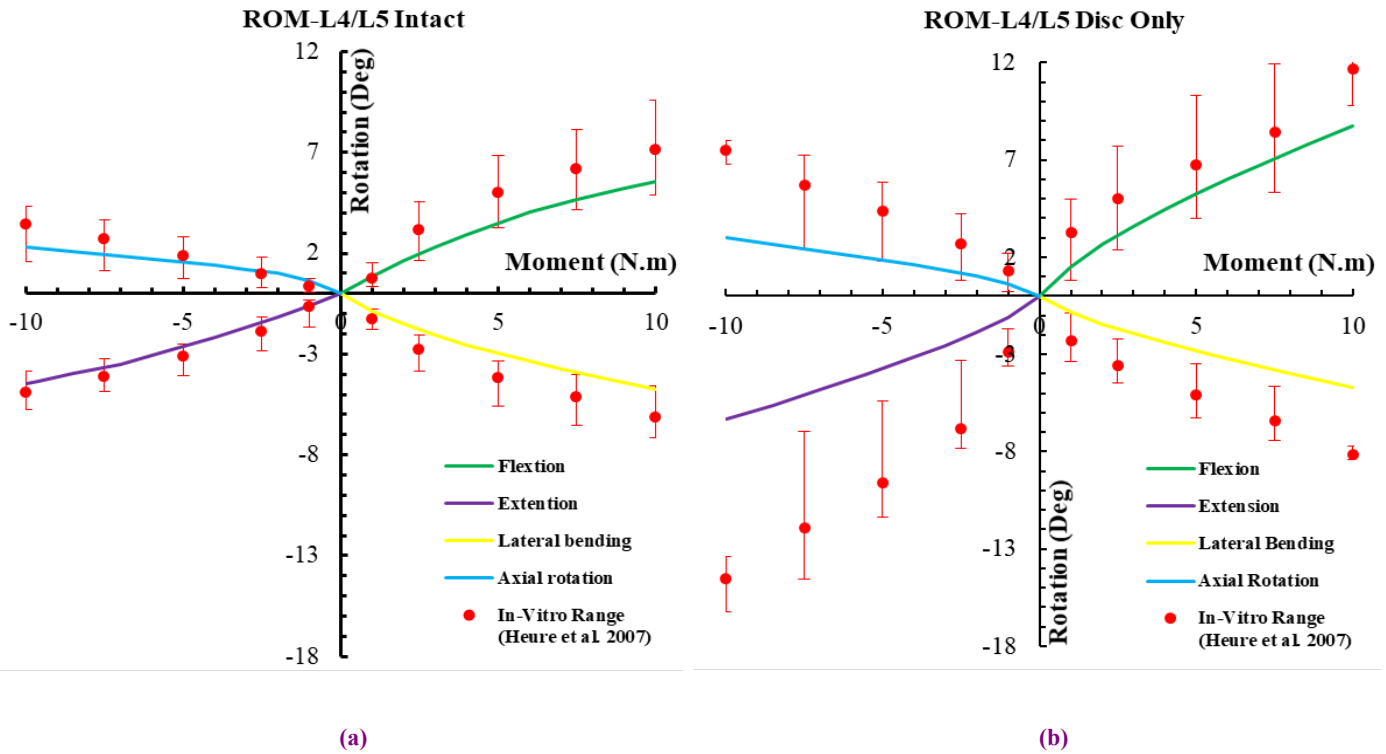


**Fig. 4. ROM for L4-L5 motion segment in different loading conditions and comparison with in-vitro data (a) Intact (b) Disc only**

and the results of ROM are obtained.

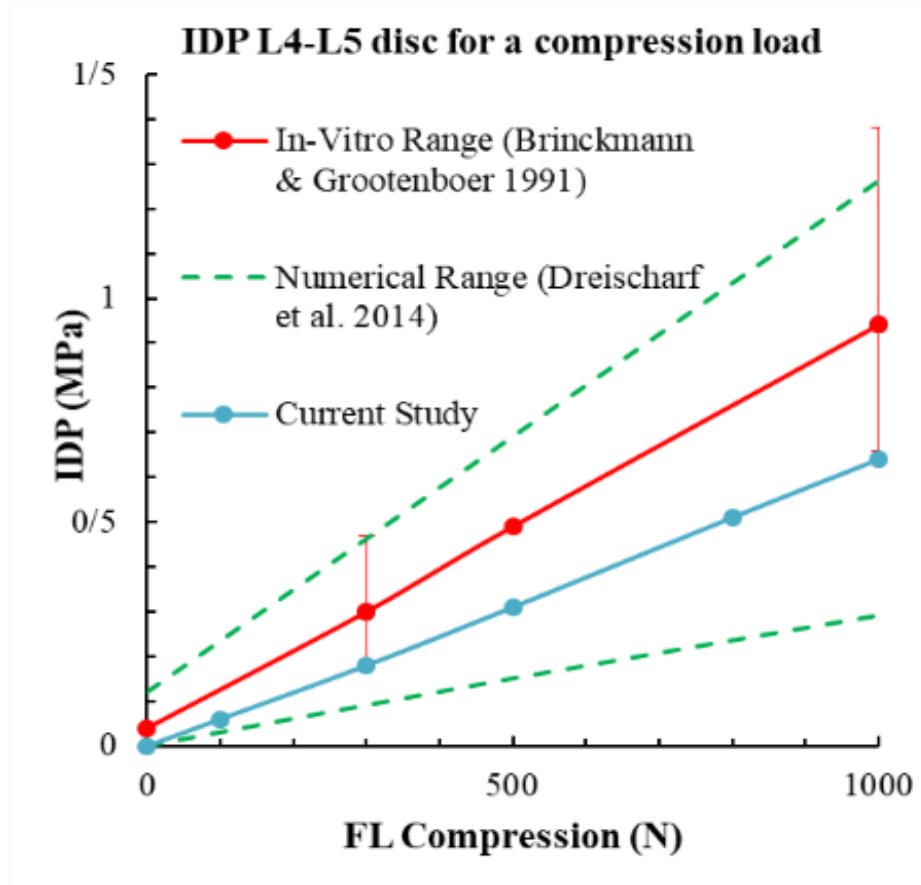
The number of disc layers as well as the elements of the whole segment together with the obtained results for each loading case are presented in Table 5. Also, Fig. 3 depicts the variation of ROM with respect to the number of elements for the intact L4-L5 motion segment.

Fig. 3. Mesh convergence study for L4-L5 segment model. As shown in Fig 3, the convergence is achieved above 5

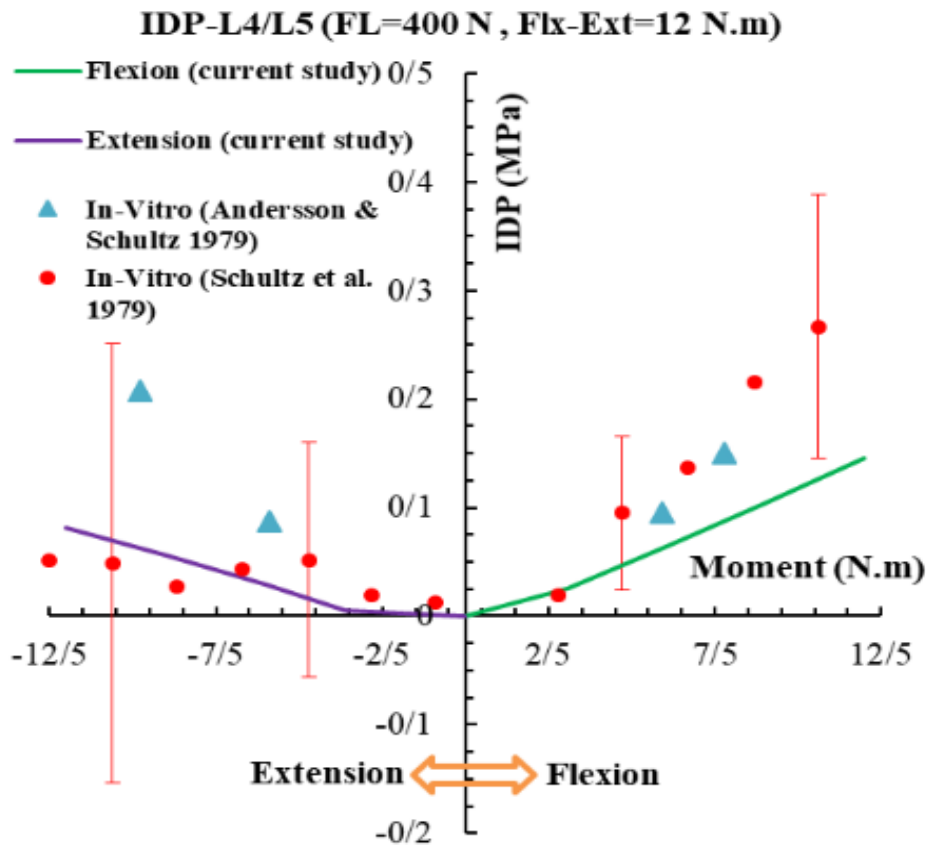
disc layers. Therefore, in this study 5 disc layers are adopted.

### 3. RESULTS AND DISCUSSION

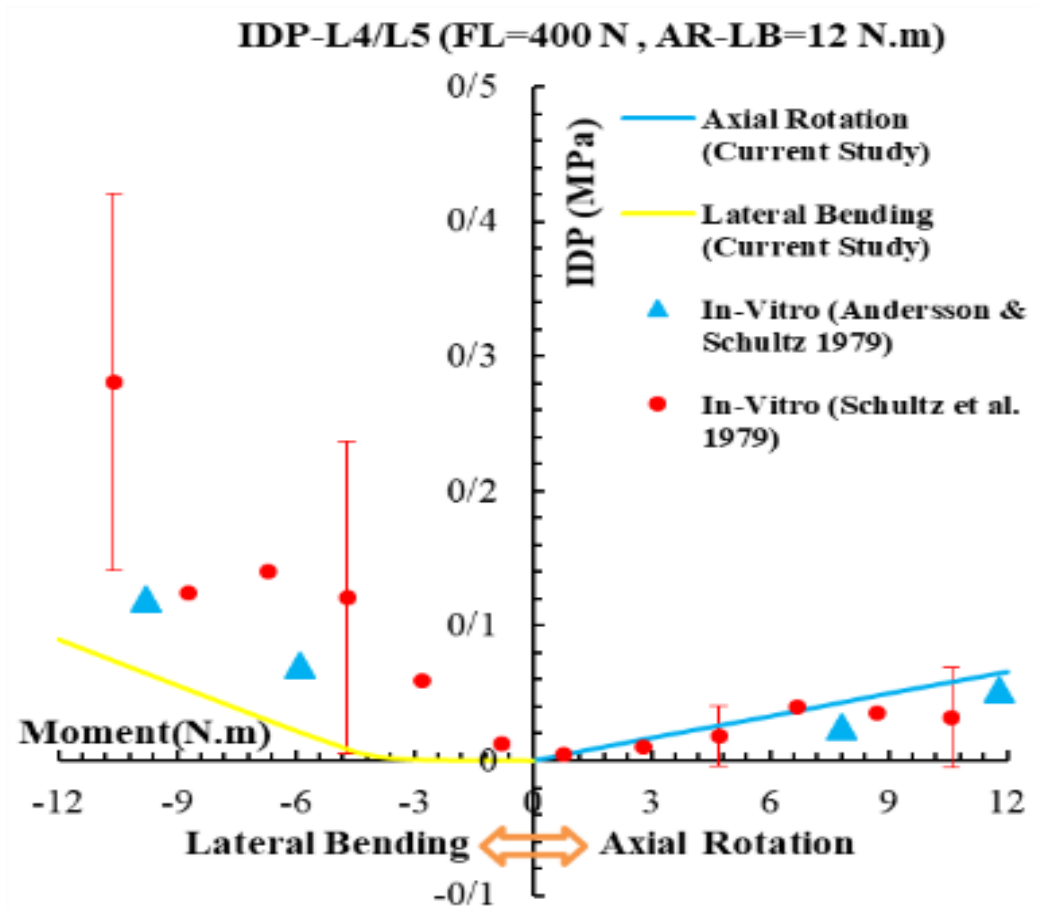
The ROM and IDP are usually considered as two determinant parameters among the parameters of the spine response to the applied external loads. The ROM shows the kinematics of the system in voluntary and involuntary movements and represents the stability of the spinal system.



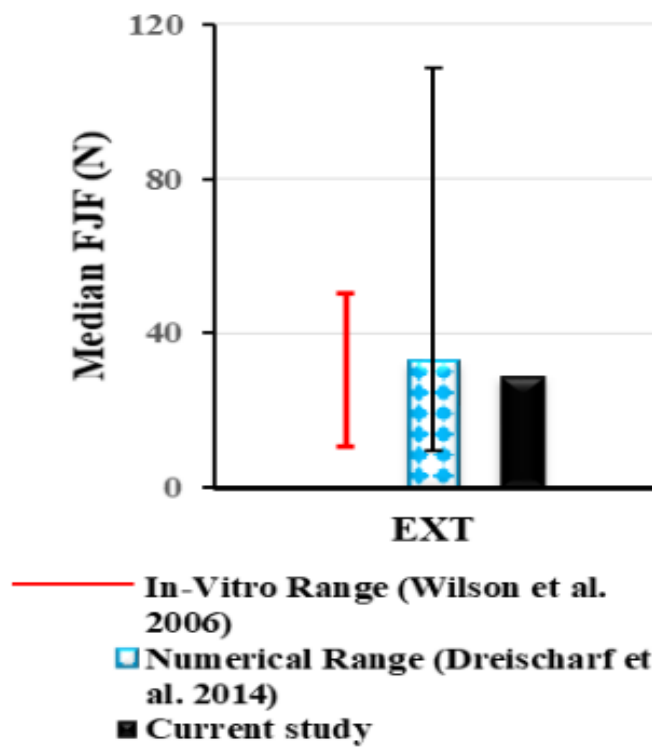
(a)



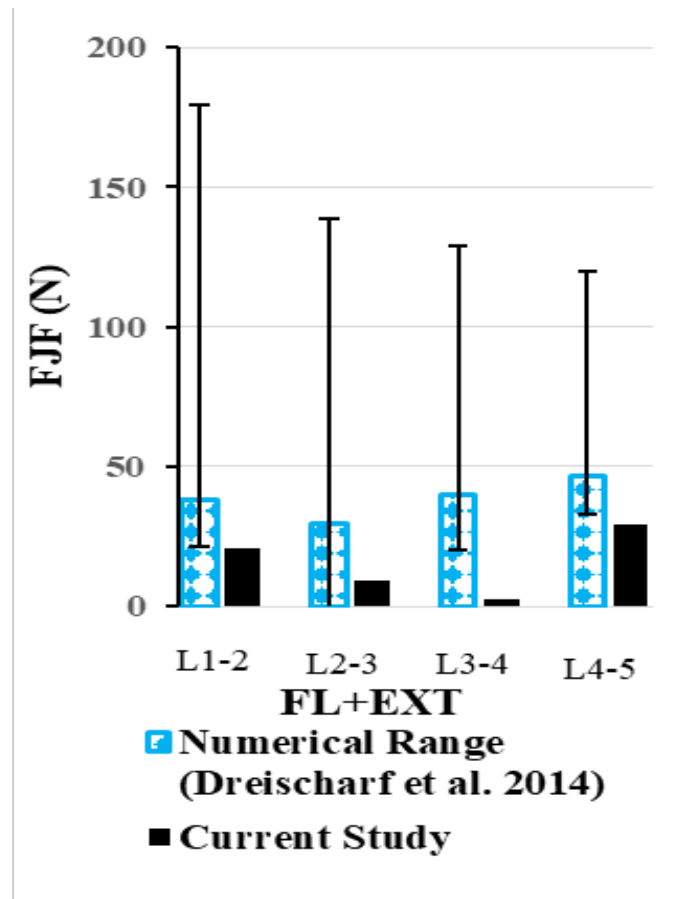
(b)



(c)



(d)



(e)

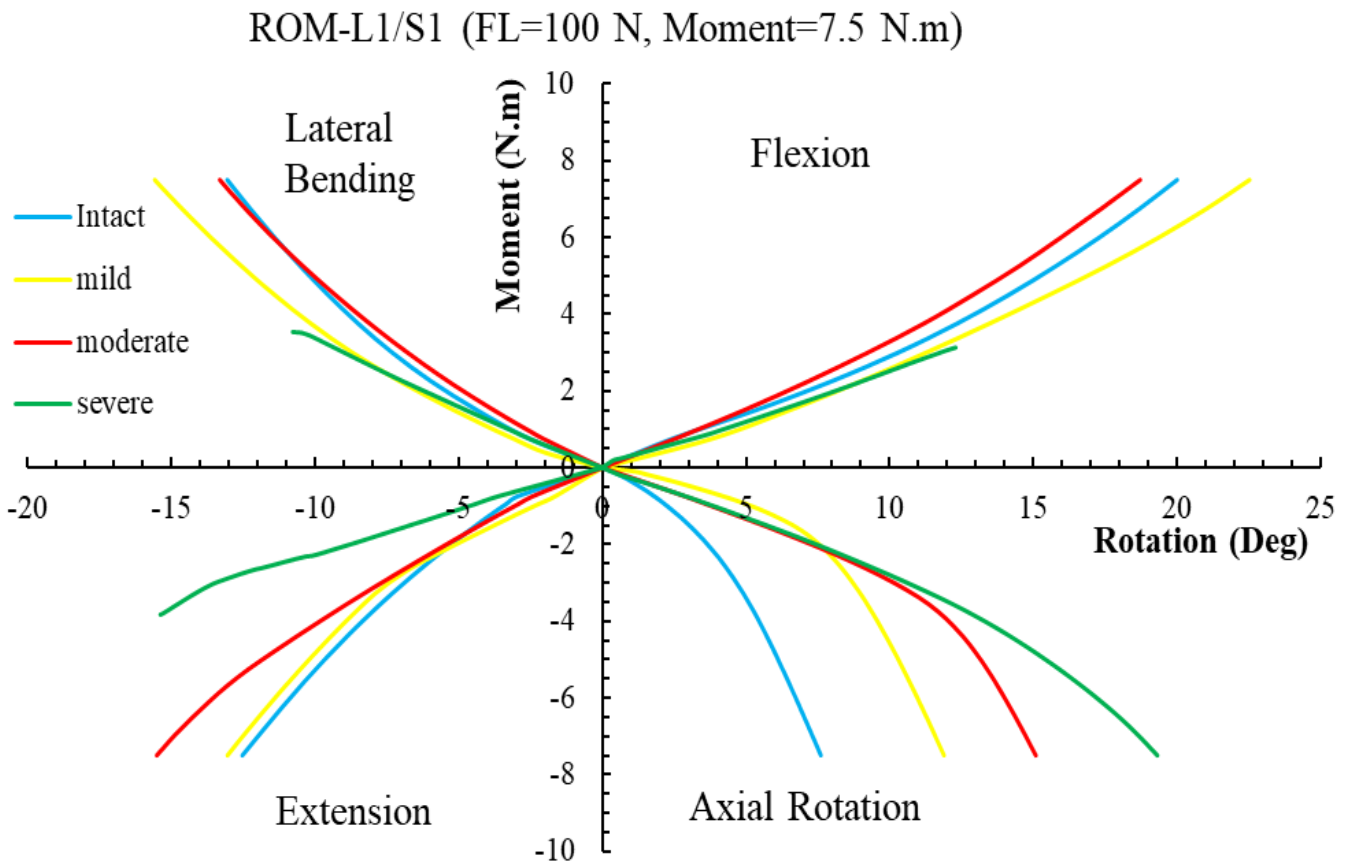
Fig. 5. The IDP of L4-L5 disc for (a) the compressive load of 1000 N, (b) the combined loading of FLX/EXT + FL, and (c) the combined loading of AR/LB + FL, (d) Median FJF in L1-L5, (e) FJF in each of the levels

Table 6. The difference of FEM results and median in vitro data in percentage

Moment (N.m)	FLX (Intact)	FLX (Disc only)	EXT (Intact)	EXT (Disc only)	AR (Intact)	AR (Disc only)	LB (Intact)	LB (Disc only)
	%	%	%	%	%	%	%	%
1	13.6	54	12.3	61.6	42.1	53.6	33.5	63.9
2.5	37.2	37.4	26	67.5	11.7	56.6	36.5	53.3
5	30	21.7	17.2	60	20.2	56.8	29.6	43.7
7.5	24.6	16.3	10.9	51.2	27	57.6	25.1	40.4
10	22.2	25.3	9.5	56.3	33.6	60	22.3	42.2

**Table 7. ROM results between three disc degeneration modes for validation**

	FE Study (this study)			Experiment Study (Mimura et al., 1994)		
	Flexion-Extension	Lateral Bending	Axial Rotation	Flexion-Extension	Lateral Bending	Axial Rotation
Mild	8.5°	7.9°	6.64°	12.5±3.5°	11.3±2.2°	2.5±1.9°
Moderate	6.14°	4.46°	8.15°	10.8±2.5°	7.9±2.7°	4±2.5°
Severe	4.5°	1.66°	6.73°	8.7±2.3°	2.5±1.9°	2.6±2.3°



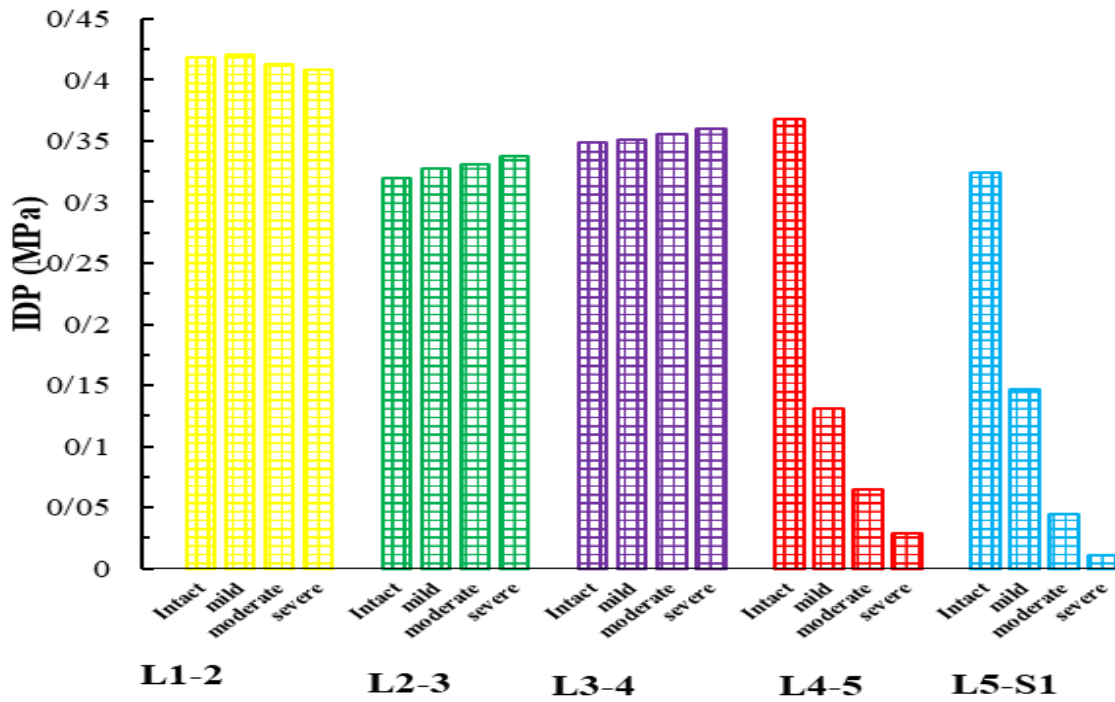
**Fig. 6. Comparison of three degeneration intervertebral rotation with intact model L1-S1 in combination loading**

The IDP, on the other hand, shows the kinetics of the system against external loads, and since the measurement of the force produced in each section of the spine is cumbersome, intradiscal pressure represents an approximate and indirect representation of these forces.

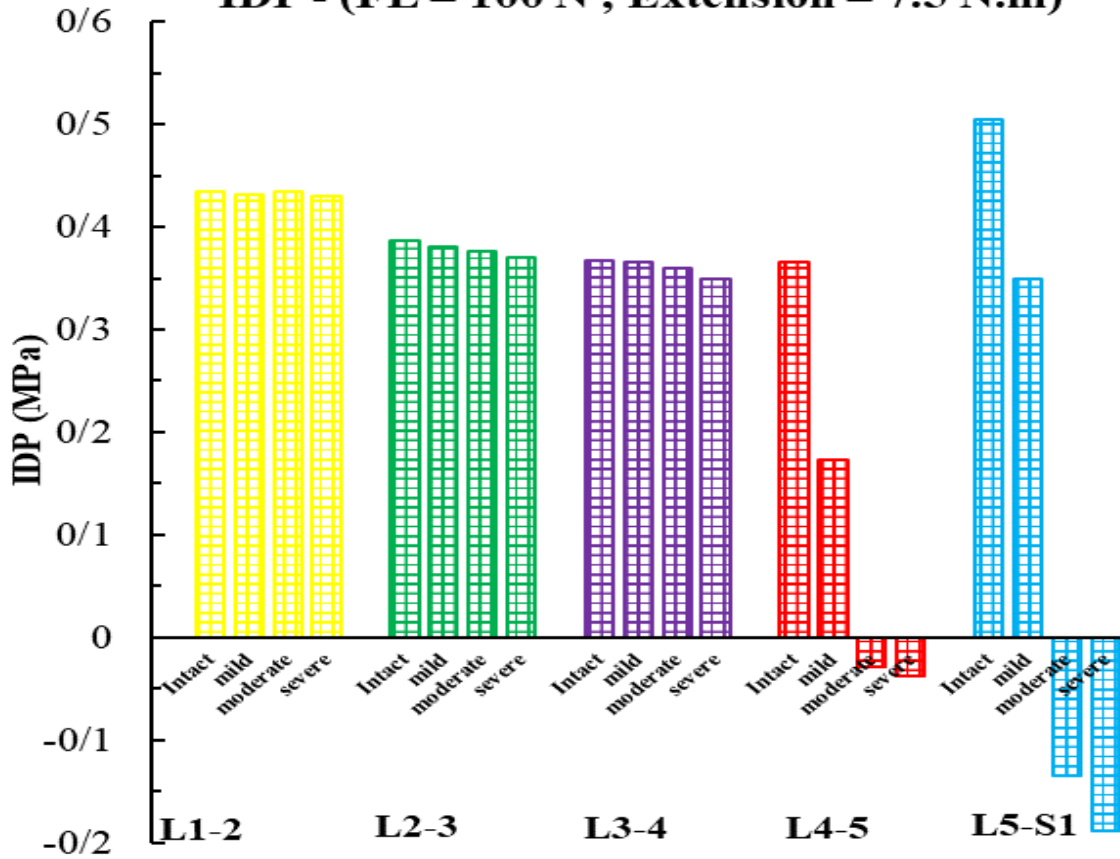
To check the reliability of the finite element model developed in this study, the modeling procedure is first

validated in two parts: a) validation of L4-L5 motion segment, in which both ROM and IDP for the healthy L4-L5 disc (disc only, without ligaments and facets) and healthy intact L4-L5 motion segment (including discs, vertebrae, ligaments, and facets) have been validated, and b) validation of L4-L5 motion segment with a degenerated disc, where ROM results are presented and compared with in-vitro data. Following the

**IDP - (FL = 100 N , Flexion = 7.5 N.m)**



**IDP - (FL = 100 N , Extension = 7.5 N.m)**



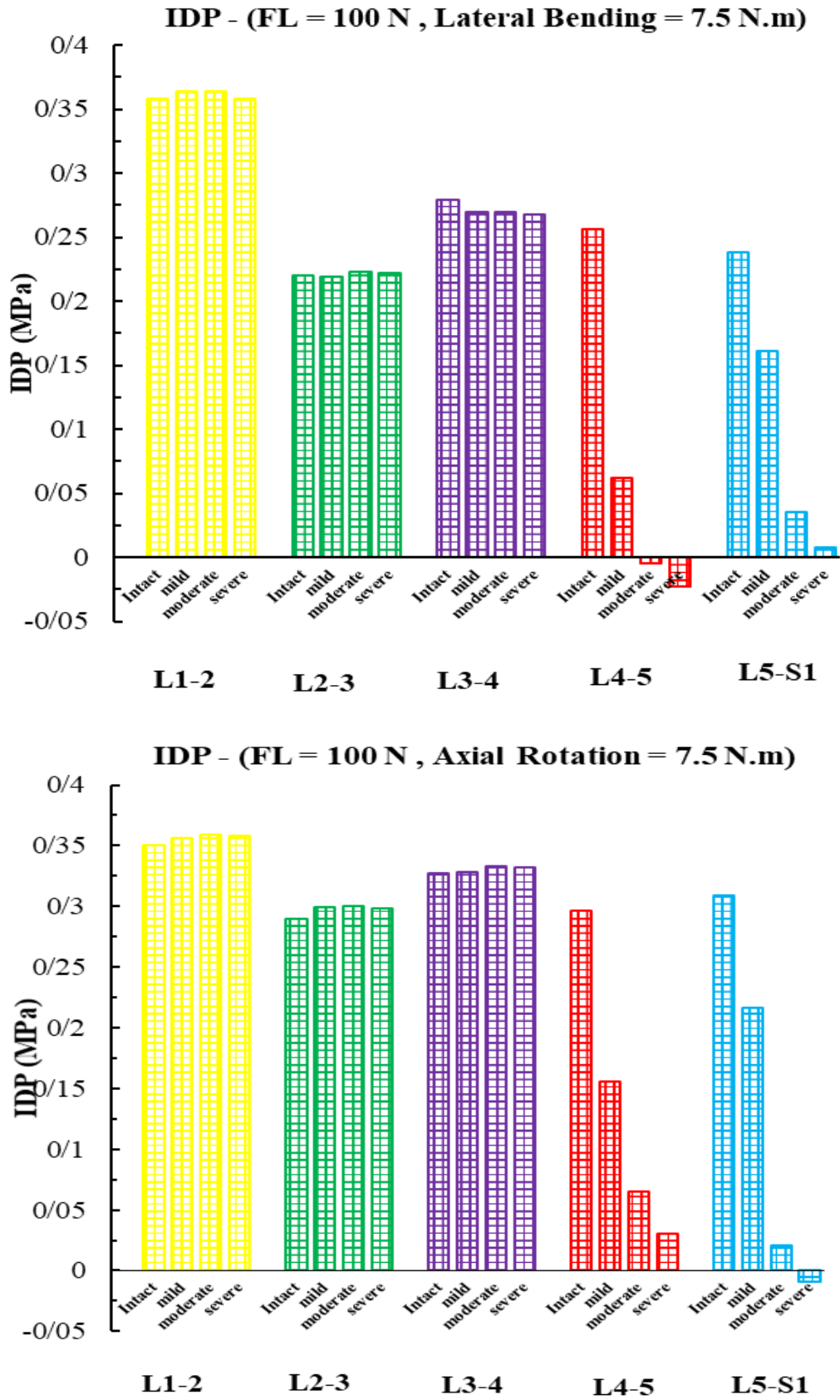
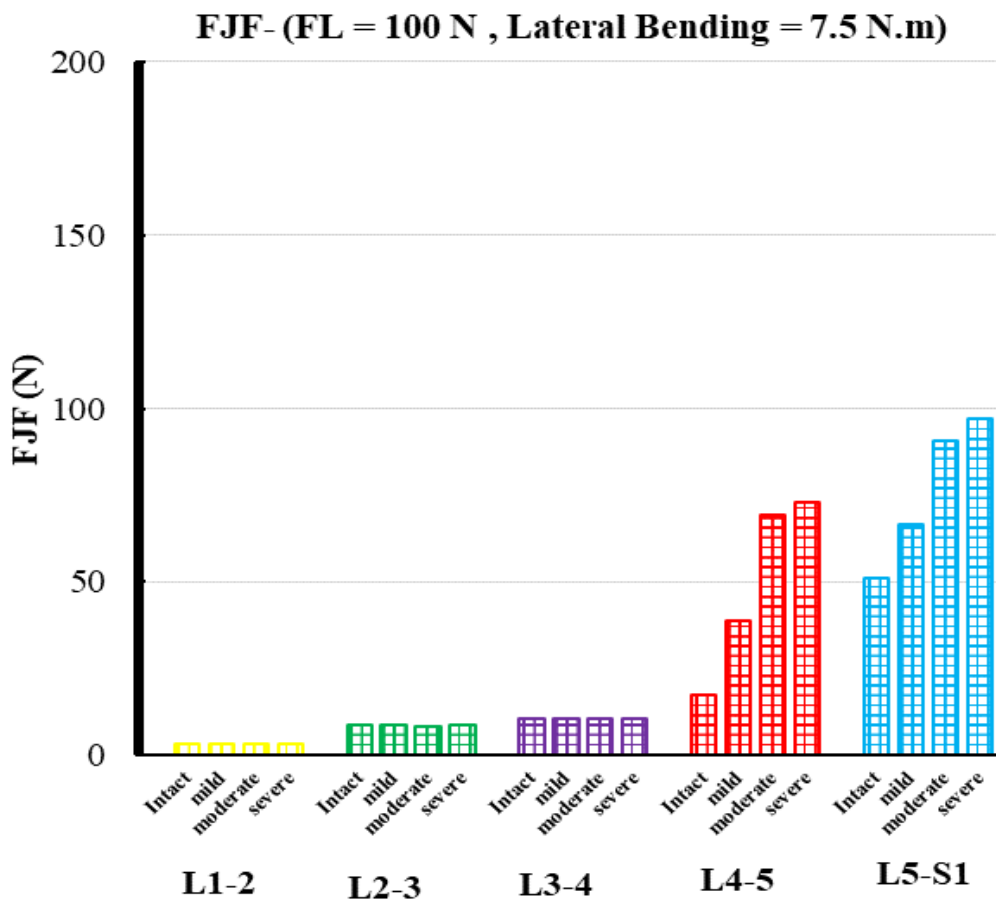
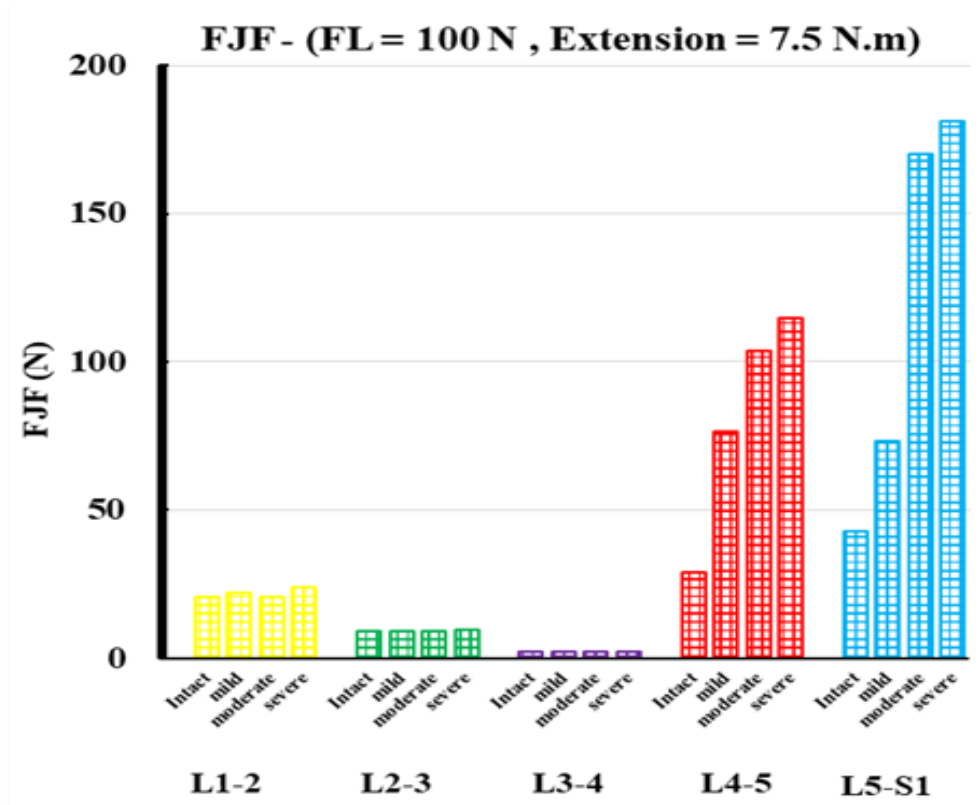
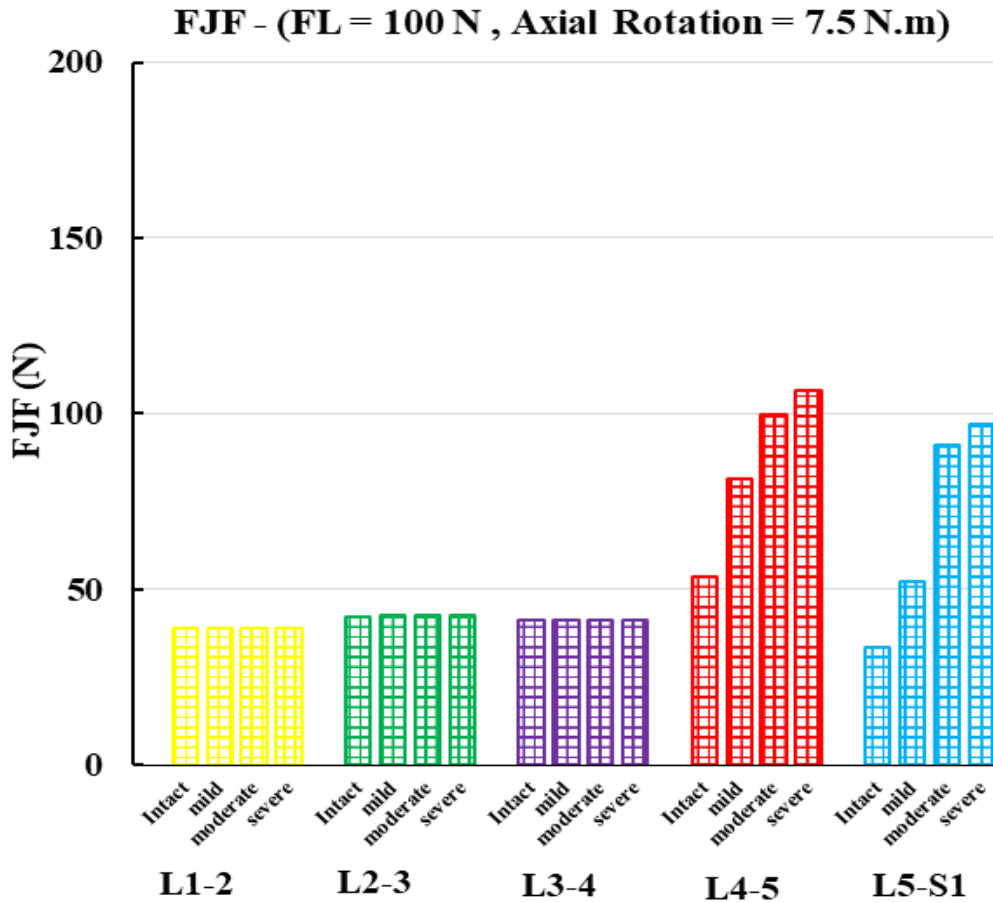


Fig. 7. Comparison of the IDP between different degeneration modes and intact mode for (a) Flexion loading (b) Extension loading (c) Lateral Bending loading (d) Axial Rotation loading





**Fig. 8. Comparison of the FJF between different degeneration modes and intact mode for loading (a) Extension loading (b) Lateral Bending loading (c) Axial Rotation loading**

validation step, the results of the double-level degeneration model of lumbar spine discs including ROM and IDP are presented.

### 3.1. Validation Step

#### 3.1.1. Validation Test Of Healthy L4-L5 Motion Segment

This geometry is, however, different from the geometry of in-vitro samples and models of other studies, in which admittedly, geometric differences and similarities are not distinguished. The L4-L5 motion segment model is then developed from the L1-S1 lumbar model by removing the L1 to L3 and S1 vertebrae and the discs associated with these vertebrae. The L4-L5 motion segment model has a fixed boundary condition at the lower endplate of the L5 vertebrae, which is exactly the same as the boundary condition applied to in-vitro samples and models of other studies. A 10 N·m moment is applied to the L4 vertebra, which is exactly the same as in-vitro samples and other numerical studies. It should be noted that since the analyses are static, even if the vertebrae L1 to L3 and the discs associated with these

vertebrae were not removed, by applying the moment to the L4 vertebra, the L4-L5 motion component could be obtained.

In Fig. 4(a), the results of ROM for the intact L4-L5 motion segment are compared with the experimental results of Heurte et al. [31]. As seen in Fig. 4(a), the results for 10 N·m moment for the loadings FLX, EXT, AR and LB are 5.55, 4.46, 2.29, and 4.76 degrees, respectively. The obtained results in this study are in the range of in-vitro data for the three cases of FLX, EXT, and AR, and for LB case touching the lower range of the experimental data.

The ROM values are also obtained when only the disc is considered. Fig. 4(b) depicts the ROM results when applying 10 N·m moment to the L4-L5 segment. The in-vitro results presented by Heurte et al. [31] are also shown in Fig. 4(b) for the purpose of comparison. In disc only case, due to ignoring ligaments and facet contacts in the modeling, the ROM is higher than the intact model in each loading case. This value was 8.73, 6.35, 3, and 7.4 degrees in FLX, EXT, AR, and LB, respectively. Anyhow, compared to the in-vitro data, the model resulted in smaller ROM while even below

the in-vitro range. As the major load-bearing component, the disc was also responsible for the relatively small ROM of the intact model. This shows that the finite element disc is stiffer than the in-vitro discs which can be due to both geometry and material property differences. In the presence of the experimental errors and the geometry and material property differences, both disc only and intact L4-L5 finite element models are stiffer than the in-vitro samples. More differences and errors have been observed in previous finite element models when compared to in-vitro data [32]. In overall and considering all loading cases the model can be considered as a reliable simulator of the lumbar spine kinematics.

To investigate the accuracy of the results of the current study, the difference of the results obtained from finite element modeling and median in vitro data is also tabulated in Table 6. The results are presented for both intact and only disc cases in L4-5 level in loading cases of FLX, EXT, AR, and LB.

As can be seen in Table 6, most of the results fall reasonably within the in-vitro data.

The validation procedure follows next by comparing the IDP values with in-vitro data. The IDP is, in fact, the average pressure at the nucleus of the disc. In fact, this pressure varies in different parts of the nucleus (not hydrostatic), and in-vivo results indicate that it is even different in two directions at one pressure point [33]. Fig. 5(a) illustrates the comparison of the results of the IDP for a 1000 N compressive load with the experimental results [34] as well as the data obtained by previous well-known finite element models [32]. As Fig. 5(a) shows, an increase in the compressive force leads to an almost linear increase in IDP. It is also seen that the results of the numerical model are almost in the range of both in-vitro data [34] and numerical models [32]. Considering the median values of IDP at 300, 500, and 1000 N, differences of 40%, 37%, and 34% are seen between the results obtained in this study and the in-vitro data. Figs. 5 (b,c) also show the results of IDP for FLX/EXT (12 N.m) plus FL (400 N) and AR/LB (12 N.m) plus FL (400 N) compared with the values of the two previous experimental studies [35, 36]. As shown in Figs. 5(b,c), it is clear that in all loading scenarios, the results are consistent with experimental data. It is known that disc cross-section area has a significant effect on the development of the IDP [37]. Although the load is the same, due to the different cross-sections, the IDP is different. That is why both in-vitro data (Fig. 5) as well as the results of previous numerical models (Fig. 5(a)) have a large dispersion. Therefore, the results obtained from the present model are relatively acceptable. Regarding these results, it can be concluded that the developed model has the potential to be applied to this study.

To validate the FJF obtained in this study, the median value of the force in L1-L5 vertebrae in the loading case of EXT has been compared with both experimental results [38] and also with the numerical range [32] (Fig. 5(d)). As can be seen in the figure, the results fall within the range of experimental data and the numerical range. The next comparison has been made for the facet joint forces obtained

in the current study and the numerical range [32] for each of the levels and the loading case of FL+EXT (Fig. 5(e)). The results for the level of L1-2 and L2-3 are within the numerical range. However, the results related to L3-4 and L4-5 levels are, respectively, 37.6 and 17.3 N different from the median value of the numerical range.

### 3.1.2. Validation Test Of L4-L5 Motion Segment With Degenerated Disc

Three disc degeneration grades (mild, moderate and severe) are modelled for the L4-L5 motion segment. The results of ROM are then compared with the in-vitro data taken from experiments of Mimura et al. [39] (Table 7). As seen in Table 7, the effect of disc degeneration on ROM is satisfactorily predicted by the developed model. Although the finite element model is stiffer (smaller ROM) in FLX-EXT, LB and more flexible in AR than the in-vitro samples, but, both the current study and the experimental data show the same pattern of degeneration effect. As disc degeneration increases, ROM in both FLX-EXT and LB loads decreases. However, in AR loading case, a monotonic decreasing trend is not seen in both experimental and finite element results. This confirms that the current model is again reliable in simulating disc degeneration and its mechanical effect on the spinal motion segment.

## 3.2. Double-Level Degeneration Mode Results

### 3.2.1. Range Of Motion Results

ROM has been obtained for a model of L1-S1 considering three degeneration grades (mild, moderate and severe) for double-level degenerated discs (L4-L5 and L5-S1 discs are simultaneously degenerated to the same grade) and the results were compared with those of the healthy disc model (Fig. 6). This comparison shows the amount of change that happens in ROM concurrently, due to the degeneration of the L4-L5 and L5-S1 discs. Experimental (in-vitro or in-vivo) data is less accessible in this case. ROM values for the healthy model in FLX, EXT, AR, and LB are 20, 12.5, 7.6 and 13.5 degrees, respectively.

As Fig. 6 shows, in AR and EXT loading, ROM values have an increasing trend with double-level degeneration mode changing from mild to severe. In AR loading, in double-level degeneration modes of mild, moderate, and severe, differences of 4.29, 7.48, and 11.71 degrees are respectively seen in ROM values as compared to the intact model. Also, in EXT loading, ROM values increase 0.52 and 2.97 degrees, respectively, in mild and moderate double-level degeneration mode when compared to the intact model. This is while an obvious trend is not seen in LB and FLX loading.

The finite element model of severely degenerated L1-S1 disc for FLX, EXT, and LB cases did not converge. In the beginning, this seemed to be due to minimum time increment, as this can be set at  $1 \times 10^{-5}$  for a static solution. However, if a time increment lower than this Min value is required, the solution does not converge. For the case of severe degeneration in loadings of FLX, EXT, and LB, the ABAQUS software stops the solution with the error message of "Time increment

required is less than the minimum specified". It should be noted, however, that due to the thickness reduction of discs in FLX, EXT, and LB loadings, bending moments higher than 3.13, 3.83, and 3.54, cannot be tolerated, respectively. In fact, the main cause of such an error can be attributed to the increase of failed elements caused by disc thickness reduction and subsequent element volume decrease.

### 3.2.2. Intradiscal Pressure

The IDP for each loading case of FLX, EXT, LB, and AR in a healthy spine and three grades of double-level degeneration (mild, moderate, and severe) is presented in Fig. 7. As shown in Fig. 7, in all four loading cases, the IDP values in L1-L2, L2-L3, and L3-L4 discs are minorly affected by double-level disc degeneration. However, the IDP values of degenerated discs (L4-L5 and L5-S1 discs) decrease significantly when the degeneration grade worsens from mild to severe. This shows that the effect of disc degeneration although significantly affects the degenerated levels but has a very minor effect on adjacent levels. This suggests that disc degeneration is independent of the mechanical performance of its adjacent levels. Although high mechanical loads accelerate the disc degeneration, degeneration does not exert additional loads on adjacent levels. One should mention that the observed effect may be true in the passive spine. If muscle activity is taken into account, there might be load changes in order to compensate for the degeneration effects which might as well affect the adjacent levels.

It is also seen that the IDP becomes negative in some modes of double-level degeneration in EXT, LB, and AR loading. Reduction of the IDP indicates the stress shielding in the motion segment. Due to disc degeneration, the disc loses much of its bulk, and thus, fails to continue its normal performance and transferring the loads. Therefore, stress shielding occurs and other spinal parts like facets take the disc share and bear the additional load. This leads to disc force reduction and decrease in IDP particularly in EXT, LB, and AR loading cases where facets contribution is significant. The in-vitro tests by Pollintine et al. [40] also showed that under the compressive loads, a healthy disc bears 92% of the load and facet bears the remaining 8%. This is while a degenerated disc bears only 60% of the load and facets have to bear the remaining 40%.

### 3.2.3. Facet Joint Force

Fig. 8 illustrates the facet joint force for the cases of EXT, LB, and AR in the lumbar spine with double-level degeneration.

The facet joint force in L4-L5 segment in the loading case of EXT has increased from 29 N in the intact case to 76, 103, and 114 N in the cases of mild, moderate, and severe degeneration, respectively. In LB loading case, as the degeneration progresses, the facet joint force experiences an increasing trend from 17 N in the intact case to 38, 70, and 73 N for the cases of mild, moderate, and severe degeneration, respectively. Also, in the case of AR loading, the facet joint force is equal to 53 N for the intact case and in the cases of mild,

moderate, and severe degeneration increases to, respectively, 81, 100, and 107 N. These increasing trends in the facet joint force indicate that the progression of degeneration causes the facet joint to increase in the degenerated discs, but no change is observed in the facet joint of adjacent segments.

The findings of the current study are believed to better clarify the biomechanics of double-level degeneration and hence clinical intervention in the patients can be better directed, especially following surgical operations such as fusion surgery.

It should be admitted that this study also includes some limitations. As mentioned in the manuscript, one of the limitations in this study is related to severe disc degeneration, in which the solution does not converge. Another limitation can be related to the geometry of the model which is for a specific person and can hardly represent the whole population. The properties of the degenerated disc are also assigned based on a theory that should be experimentally verified in future studies.

## 4. CONCLUSIONS

Low back pain is the most common type of back pain and one of the most common musculoskeletal disorders in modern societies. Through various clinical and radiological studies, it has been shown that the degeneration of the disc can be one of the major causes of back pain. Although there is no precise data concerning the rate of degeneration in Iran, the statistics show a wide range of issues in other parts of the world.

Therefore, the effect of disc degeneration was examined on computational parameters of the spine using a nonlinear FE model developed in this study. The analysis of the results of double-level degeneration (where two adjacent discs are degenerated), which is a special case of disc degeneration, is presented here. Due to the prevalence of degeneration in the L4-5 and L5-S1 discs, degeneration is modeled simultaneously for these two discs. The results showed that in EXT and AR loading, the ROM increases with an increase in disc degeneration. This is while in FLX and LB loading, ROM intersect in mild degeneration. Degeneration of the L4-5 and L5-S1 discs does not have a significant effect on the IDP of other adjacent discs. However, degeneration of these two discs would lead to the reduction of their IDP.

Results indicate changes in load-sharing between different spinal structures (e.g. discs and facets) due to disc degeneration. That is disc degeneration may result in an increased risk of injury to other tissues such as facet joints. Future studies will focus on designing surgery techniques to balance this load-sharing. Our research group plans to modify the current FEM model to address these limitations in future studies and also extend the FEM model.

## REFERENCES

- [1] D.I. Rubin, Epidemiology and risk factors for spine pain, *Neurologic clinics*, 25(2) (2007) 353-371.
- [2] V.M. Ravindra, S.S. Senglaub, A. Rattani, M.C. Dewan, R. Härtl, E. Bisson, K.B. Park, M.G. Shrimel, Degenerative lumbar spine disease: estimating global incidence and worldwide volume, *Global spine*

- journal, 8(8) (2018) 784-794.
- [3] J.A. Miller, C. Schmatz, A. Schultz, Lumbar disc degeneration: correlation with age, sex, and spine level in 600 autopsy specimens, *Spine*, 13(2) (1988) 173-178.
- [4] Y. Kim, V.K. Goel, J.N. Weinstein, T.-h. Lim, Effect of disc degeneration at one level on the adjacent level in axial mode, *Spine*, 16(3) (1991) 331-335.
- [5] A. Polikeit, L.P. Nolte, S.J. Ferguson, Simulated influence of osteoporosis and disc degeneration on the load transfer in a lumbar functional spinal unit, *Journal of biomechanics*, 37(7) (2004) 1061-1069.
- [6] L.N. Omran, K.A. Ezzat, M. Elhoseny, A.E. Hassanien, Biomechanics of artificial intervertebral disc with different materials using finite element method, *Soft Computing*, 23(19) (2019) 9215-9236.
- [7] H. Schmidt, A. Kettler, A. Rohlmann, L. Claes, H.-J. Wilke, The risk of disc prolapses with complex loading in different degrees of disc degeneration—a finite element analysis, *Clinical biomechanics*, 22(9) (2007) 988-998.
- [8] A. Rohlmann, T. Zander, H. Schmidt, H.-J. Wilke, G. Bergmann, Analysis of the influence of disc degeneration on the mechanical behaviour of a lumbar motion segment using the finite element method, *Journal of biomechanics*, 39(13) (2006) 2484-2490.
- [9] M.D. Brown, D.C. Holmes, A.D. Heiner, Measurement of cadaver lumbar spine motion segment stiffness, *Spine*, 27(9) (2002) 918-922.
- [10] L.M. Ruberté, R.N. Natarajan, G.B. Andersson, Influence of single-level lumbar degenerative disc disease on the behavior of the adjacent segments—a finite element model study, *Journal of Biomechanics*, 42(3) (2009) 341-348.
- [11] I. Dehghan-Hamani, N. Arjmand, A. Shirazi-Adl, Subject-specific loads on the lumbar spine in detailed finite element models scaled geometrically and kinematic-driven by radiography images, *International journal for numerical methods in biomedical engineering*, 35(4) (2019) e3182.
- [12] W.M. Park, K. Kim, Y.H. Kim, Effects of degenerated intervertebral discs on intersegmental rotations, intradiscal pressures, and facet joint forces of the whole lumbar spine, *Computers in biology and medicine*, 43(9) (2013) 1234-1240.
- [13] Y. Wu, Y. Wang, J. Wu, J. Guan, N. Mao, C. Lu, R. Lv, M. Ding, Z. Shi, B. Cai, Study of double-level degeneration of lower lumbar spines by finite element model, *World neurosurgery*, 86 (2016) 294-299.
- [14] R.M. Kanna, A.P. Shetty, S. Rajasekaran, Patterns of lumbar disc degeneration are different in degenerative disc disease and disc prolapse magnetic resonance imaging analysis of 224 patients, *The Spine Journal*, 14(2) (2014) 300-307.
- [15] S.-H. Lee, S.D. Daffner, J.C. Wang, Does lumbar disk degeneration increase segmental mobility in vivo?: segmental motion analysis of the whole lumbar spine using kinetic MRI, *Clinical Spine Surgery*, 27(2) (2014) 111-116.
- [16] M. El-Rich, P.-J. Arnoux, E. Wagnac, C. Brunet, C.-E. Aubin, Finite element investigation of the loading rate effect on the spinal load-sharing changes under impact conditions, *Journal of biomechanics*, 42(9) (2009) 1252-1262.
- [17] H. Schmidt, A. Kettler, F. Heuer, U. Simon, L. Claes, H.-J. Wilke, Intradiscal pressure, shear strain, and fiber strain in the intervertebral disc under combined loading, *Spine*, 32(7) (2007) 748-755.
- [18] H. Schmidt, F. Heuer, U. Simon, A. Kettler, A. Rohlmann, L. Claes, H.-J. Wilke, Application of a new calibration method for a three-dimensional finite element model of a human lumbar annulus fibrosus, *Clinical Biomechanics*, 21(4) (2006) 337-344.
- [19] C. Breau, A. Shirazi-Adl, J. De Guise, Reconstruction of a human ligamentous lumbar spine using CT images—a three-dimensional finite element mesh generation, *Annals of biomedical engineering*, 19(3) (1991) 291-302.
- [20] U.M. Ayturk, C.M. Puttlitz, Parametric convergence sensitivity and validation of a finite element model of the human lumbar spine, *Computer methods in biomechanics and biomedical engineering*, 14(8) (2011) 695-705.
- [21] S. Naserkhaki, J.L. Jaremko, S. Adeeb, M. El-Rich, On the load-sharing along the ligamentous lumbosacral spine in flexed and extended postures: finite element study, *Journal of biomechanics*, 49(6) (2016) 974-982.
- [22] T. Liu, K. Khalaf, S. Naserkhaki, M. El-Rich, Load-sharing in the lumbosacral spine in neutral standing & flexed postures—A combined finite element and inverse static study, *Journal of biomechanics*, 70 (2018) 43-50.
- [23] S. Naserkhaki, N. Arjmand, A. Shirazi-Adl, F. Farahmand, M. El-Rich, Effects of eight different ligament property datasets on biomechanics of a lumbar L4-L5 finite element model, *Journal of biomechanics*, 70 (2018) 33-42.
- [24] H. Schmidt, F. Heuer, J. Drumm, Z. Klezl, L. Claes, H.-J. Wilke, Application of a calibration method provides more realistic results for a finite element model of a lumbar spinal segment, *Clinical biomechanics*, 22(4) (2007) 377-384.
- [25] A. Shirazi-Adl, A.M. Ahmed, S.C. Shrivastava, Mechanical response of a lumbar motion segment in axial torque alone and combined with compression, *Spine*, 11(9) (1986) 914-927.
- [26] A. Shirazi-Adl, A.A.S.S. Spine, Mechanical response of a lumbar motion segment in axial torque alone and combined with compression, *Clinical Biomechanics*, 2(3) (1987).
- [27] R.W. Fry, T.F. Alamin, L.I. Voronov, L.C. Fielding, A.J. Ghanayem, A. Parikh, G. Carandang, B.W. McIntosh, R.M. Havey, A.G. Patwardhan, Compressive preload reduces segmental flexion instability after progressive destabilization of the lumbar spine, *Spine*, 39(2) (2014) E74-E81.
- [28] S.M. Renner, R.N. Natarajan, A.G. Patwardhan, R.M. Havey, L.I. Voronov, B.Y. Guo, G.B. Andersson, H.S. An, Novel model to analyze the effect of a large compressive follower pre-load on range of motions in a lumbar spine, *Journal of Biomechanics*, 40(6) (2007) 1326-1332.
- [29] S. Naserkhaki, J.L. Jaremko, G. Kawchuk, S. Adeeb, M. El-Rich, Investigation of lumbosacral spine anatomical variation effect on load-partitioning under follower load using geometrically personalized finite element model, in: *ASME 2014 International Mechanical Engineering Congress and Exposition*, American Society of Mechanical Engineers, 2014, pp. V003T003A050-V003T003A050.
- [30] H.-J. Wilke, S. Wolf, L.E. Claes, M. Arand, A. Wiesend, Stability increase of the lumbar spine with different muscle groups. A biomechanical in vitro study, *Spine*, 20(2) (1995) 192-198.
- [31] F. Heuer, H. Schmidt, Z. Klezl, L. Claes, H.-J. Wilke, Stepwise reduction of functional spinal structures increase range of motion and change lordosis angle, *Journal of biomechanics*, 40(2) (2007) 271-280.
- [32] M. Dreischarf, T. Zander, A. Shirazi-Adl, C. Puttlitz, C. Adam, C. Chen, V. Goel, A. Kiapour, Y. Kim, K. Labus, Comparison of eight published static finite element models of the intact lumbar spine: predictive power of models improves when combined together, *Journal of biomechanics*, 47(8) (2014) 1757-1766.
- [33] K. Sato, S. Kikuchi, T. Yonezawa, In vivo intradiscal pressure measurement in healthy individuals and in patients with ongoing back problems, *Spine*, 24(23) (1999) 2468.
- [34] P. Brinckmann, H. Grootenboer, Change of disc height, radial disc bulge, and intradiscal pressure from discectomy. An in vitro investigation on human lumbar discs, *Spine*, 16(6) (1991) 641-646.
- [35] G.B. Andersson, A.B. Schultz, Effects of fluid injection on mechanical properties of intervertebral discs, *Journal of biomechanics*, 12(6) (1979) 453-458.
- [36] A. Schultz, D. Warwick, M. Berkson, A. Nachemson, Mechanical properties of human lumbar spine motion segments—Part I: responses in flexion, extension, lateral bending, and torsion, *Journal of Biomechanical Engineering*, 101(1) (1979) 46-52.
- [37] M. Dreischarf, A. Rohlmann, R. Zhu, H. Schmidt, T. Zander, Is it possible to estimate the compressive force in the lumbar spine from

intradiscal pressure measurements? A finite element evaluation, *Medical engineering & physics*, 35(9) (2013) 1385-1390.

[38] D.C. Wilson, C.A. Niosi, Q.A. Zhu, T.R. Oxland, D.R. Wilson, Accuracy and repeatability of a new method for measuring facet loads in the lumbar spine, *Journal of biomechanics*, 39(2) (2006) 348-353.

[39] M. Mimura, M. Panjabi, T. Oxland, J. Crisco, I. Yamamoto, A. Vasavada,

Disc degeneration affects the multidirectional flexibility of the lumbar spine, *Spine*, 19(12) (1994) 1371-1380.

[40] P. Pollintine, P. Dolan, J.H. Tobias, M.A. Adams, Intervertebral disc degeneration can lead to "stress-shielding" of the anterior vertebral body: a cause of osteoporotic vertebral fracture?, *Spine*, 29(7) (2004) 774-782.

#### HOW TO CITE THIS ARTICLE

A. Orang, M. Haghghi-Yazdi, S. R. Mehrpour, *Mechanical effect of double-level degeneration of lumbar spine discs by finite element method*, *AUT J. Mech. Eng.*, 5(1) (2021) 77-96,

DOI: [10.22060/ajme.2020.16442.5818](https://doi.org/10.22060/ajme.2020.16442.5818)



